# A Combination Approach for 2-D Interference Channel Based on Factor Graph in BPMR System

**Thanomsak Sopon** [1†] and **Pornchai Supnithi** [2], Non-members

**ABSTRACT**

High areal density in bit-patterned media recording (BPMR) systems encounters several challenges, such as two-dimensional (2-D) interference channels and media noises in the presence of severe fluctuations. To combat the effects of the 2-D interference channel, a factor graph-based detector (FGB) is one of the promising detectors for the 2-D detection that can mitigate the channel impairment. In this paper, we propose an improvement of factor graph decoding for 2-D interference channels of the BPMR system. The 2-D interference channel is separated into the two targets that are the upper triangular target and the lower triangular target. After that, the joint outputs are averaged for each detector. The simulation results show that the proposed FGB detector method achieves lower bit error rate (BER) performances than both the conventional FGB detector and the 2-D FGB detector on the BPMR system with an areal density of 3 and 4 Tb/in$^2$.

**Keywords**: Information storage, bit patterned media recording, 2-D interference channel, factor graph-based detector

## 1. INTRODUCTION

In the magnetic recording system, the bit-patterned media recording (BPMR) system is considered magnetic recording technology for high areal density magnetic storage of the hard disk drives (HDD). The BPMR system stores each bit in single-domain islands [1-5]. In the present study, the BPMR system is a promising technology for achieving areal densities of more than 5 Tb/in$^2$ [6-9]. The higher areal density of BPMR accomplished by reducing the bit islands (or grain sizes) causes a lower signal-to-noise ratio (SNR) as well as more severe interferences. The reduction of grain sizes in both across-track and along-track directions leads to the 2-D interference consisting of inter-symbol interferences (ISI) and inter-track interferences (ITI) from the adjacent tracks [10-12]. Moreover, the effects of fluctuations of island size and the position result in the media noise, which degrades the performance of the read channels [13-17].

In a previous study, to resolve problems such as 2-D interference channels and media noise, many researchers have introduced 2-D detection schemes to improve the BER performance for the BPMR channel. Therefore, there has been some important work on 2-D detection for 2-D interference channels and magnetic recording systems. For example, an iterative 2-D soft-output Viterbi algorithm (SOVA) detector based on the 2-D equalization followed by 1-D detectors in both directions is proposed [18]. The 2-D SOVA detector separately processes the 1-D SOVA detector in the horizontal and vertical directions. The iterative 2-D SOVA detector is the conventional SOVA detector with the 1-D SOVA detector of each direction. In [19], the researchers presented the scheme with joint-track equalization based on the Viterbi detector with the modified branch metric on a 4-state trellis. In [20], the twin iterative detection scheme based on a 1-D detector and decoders was proposed. The iterative detector was separately carried out between the decoder and 1-D detector in each direction. Y. Wang *et al.* [21] proposed a variable 2-D equalizer whose equalizer coefficients and corresponding partial response (PR) targets depend on the different ITI patterns. They modified multi-track detection with a hybrid 2-D equalizer and Viterbi algorithm detector. S. Jeong *et al.* [23] proposed a three-path (3P) SOVA of investigated different partial response targets to compare the BER performances of detection schemes: the 1-D SOVA, 2-D SOVA, and 3P SOVA. In [24], they proposed an iterative parallel-serial structure of the detection based on the maximum a posteriori (MAP) algorithm with extracted extrinsic information from the outputs.

To mitigate the effects of the 2-D inter-symbol interference channel with multi-track recording, a graph-based channel detection is an alternative to the 2-D detection [25-26]. Thereby, the factor graph-based (FGB) detector is employed instead of the multi-dimensional Viterbi algorithm detector. The FGB detection is based on message passing of *a posteriori* log-likelihood ratio (LLR) information between factor nodes and bit nodes. However, previous works on FGB detections are still complex as the graph is constructed from the 2-D interference channels [27-28]. Additionally, S. M. Khatami, *et al.* [29] proposed a new framework for designing generalized belief propagation (GBP) algorithm [30] on

Manuscript received on June 15, 2024; revised on July 15, 2024; accepted on August 5, 2024. This paper was recommended by Associate Editor Yodchanan Wongsawat.

[1]The author is with Faculty of Engineering and Technology, Rajamangala University of Technology Isan, Nakhon Ratchasima 30000, Thailand.

[2]The author is with School of Engineering, King Mongkut's Institute of Technology Ladkrabang, Bangkok 10520, Thailand.

[†]Corresponding author: thanomsak.so@rmuti.ac.th



Digital Object Identifier: 10.37936/ecti-eec.2525231.254399

the two-dimensional magnetic recording (TDMR) micro-cell model with severe 2-D inter-symbol interference. However, all these detection schemes are multi-head, multi-track, and there have been several important works on 2-D detection and 2-D equalization for magnetic recording channels.

In the article presented here, we used the method to improve 2-D interference channels based on the factor graph for the FGB detector on the BPMR system with multi-head, multi-track processing. The method segments the 2-D interference channel into two targets, an upper triangular target and a lower triangular target. Because the usefulness of the method is seen from its application to capacity analysis, design, and evaluation of optimized detection schemes. Such a method should reliably reflect the essential physics of the detection processes of the 2-D interference channel.

The article is divided into the following sections: the introduction of the BPMR channel model in Section II, the proposed improvement of the 2-D interference channel in the factor graph for combining the FGB detector, Section III. We perform the simulation results in Section IV. Finally, Section V concludes the paper.

## 2. BPMR CHANNEL MODEL

In this section, we present a scheme of write-read channel for the BPMR system with multi-head, multi-track processing. In a BPMR system, we assume a sequence of $[a_{j,k-2},\ a_{j,k-1},\ a_{j,k},\ a_{j,k+1},\ a_{j,k+2}]$ five information bits and recorded on five adjacent tracks for the patterned media. Hence, three read- heads will receive a sequence of three read-back signals $[r_{j,k-1}, r_{j,k}, r_{j,k+1}]$ that are caused by a combination of noiseless received signals $[y_{j,k-1}, y_{j,k}, y_{j,k+1}]$ with additive white Gaussian noise (AWGN) $[n_{j,k-1}, n_{j,k}, n_{j,k+1}]$. From track ($k$-1) and ($k$+1) are just the ITI effects for the read-back signal of the track ($k$). Next, the read-back signal sequences $[r_{j,k-1},\ r_{j,k},\ r_{j,k+1}]$ will be sent to two 2-D equalizers [33-35]. Then output bits of the 2-D equalizer will be performed between the FGB detector with the upper triangular target $[d(u)_{j,k}]$ and the FGB detector with the lower triangular target $[d(l)_{j,k}]$. Lastly, the output bit is averaged by the FGB detector with the upper triangular target and the FGB detector with the lower triangular target after the iterations, which are estimated input bit sequences $[\hat{a}_{j,k}]$, as shown in Fig. 1.

Since for a 2-D Channel [21], [31], we recall that the 2-D interference channel target or 2-D generalized partial response (GPR) target of the BPMR system with multi-track processing. Theoretically, we consider a 2-D Gaussian pulse response $h(m,n)$ following the set of equations

$$h(m,n) = (A+\Lambda_A)\exp\left\{-e\left(\frac{mT_x+\Lambda_x}{PW_{50x}}\right)^2 - g\left(\frac{nT_z+\Lambda_z}{PW_{50z}}\right)^2\right\} \tag{1}$$

where $A$ is the peak amplitude of the pulse response,

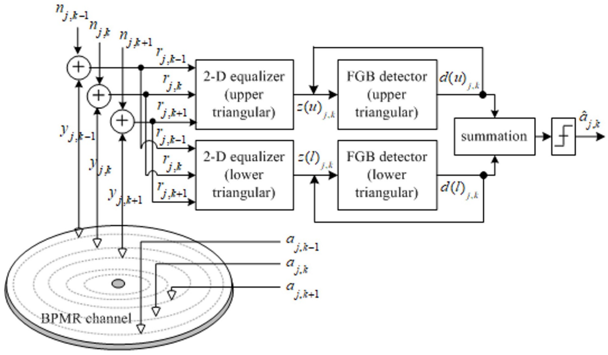


***Fig. 1**: A write-read channel on BPMR system with 2-D equalizers and improved FGB detectors.*

$\Lambda_A$ is an amplitude fluctuation, $T_x$ is the bit period in an along-track direction, and $T_z$ is the track pitch in an across-track direction. $PW_{50x}$ and $PW_{50z}$ are the widths of the Gaussian pulse at half the peak height in the along-track and across-track directions, respectively. $\Lambda_x$ and $\Lambda_z$ position fluctuations are truncated Gaussian probability density functions with zero mean in the along-track and across-track directions, respectively. The values of parameters $e = 0.35$ and $g = 0.4$ are the fitting parameters related to the geometry of the bit islands and magnetic reader. Therefore, 3 by 3 array coefficients of the 2-D interference channel from Equation (1) can be generated as

$$\mathbf{H} = \begin{bmatrix} h_{j-1,k-1} & h_{j,k-1} & h_{j+1,k-1} \\ h_{j-1,k} & h_{j,k} & h_{j+1,k} \\ h_{j-1,k+1} & h_{j,k+1} & h_{j+1,k+1} \end{bmatrix}. \tag{2}$$

where $\mathbf{H}$ is the 3×3 matrix of a symmetric 2-D interference channel target with the elements as follows: $h_{j,k}$ is the main bit coefficient, $h_{j-1,k}$ and $h_{j+1,k}$ are the inter-symbol interference coefficients, $h_{j,k-1}$ and $h_{j,k+1}$ are the inter-track interference coefficients from the adjacent tracks, and $h_{j-1,k-1}$, $h_{j-1,k+1}$, $h_{j+1,k-1}$, and $h_{j+1,k+1}$ are the cornered inter-track interference coefficients.

Afterward, the received three read-back signals $[r_{j,k-1},\ r_{j,k},\ r_{j,k+1}]$ from three read-heads, which are combined of three received signals $[y_{j,k-1},\ y_{j,k},\ y_{j,k+1}]$ and three AWGN $[n_{j,k-1},\ n_{j,k},\ n_{j,k+1}]$ due to the read head and electronics. Then the read-back signal $[r_{j,k}]$ samples obtained from the 2-D channel model, the discrete-time signal can be computed as

$$r_{j,k} = \sum_{m=-M}^{M}\sum_{n=-N}^{N} a_{j-m,k-nh_{m,n}} + n_{j,k} \tag{3}$$

where $a_{j,k}$ is random uncoded binary input bits, $h_{m,n}$ is the 2-D discrete island response of the 2-D interference channel coefficient, which covers (2$M$+1) bits and (2$N$+1) tracks, $m$ is the width of the 2-D channel in the across-track direction, and $n$ is the length of the 2-D channel in the along-track direction.

For the 2-D channel with a 3×3 matrix span, it contains 9 bits, $m$ = -1, 0, 1, and $n$ = -1, 0, 1. When expanding the preceding read-back signal equation, which is rewritten here for convenience:

$$r_{j,k} = \left(a_{j-1,k-1}h_{j-1,k-1} + a_{j-1,k}h_{j-1,k} + a_{j-1,k+1}h_{j-1,k+1}\right) + \left(a_{j,k-1}h_{j,k-1} + a_{j,k}h_{j,k} + a_{j,k+1}h_{j,k+1}\right) + \left(a_{j+1,k-1}h_{j+1,k-1} + a_{j+1,k}h_{j+1,k} + a_{j+1,k+1}h_{j+1,k+1}\right) + n_{j,k} \quad (4)$$

## 3. FACTOR GRAPH-BASED DETECTION

Factor graph-based (FGB) detection is a factor graph that can use a belief propagation algorithm for computing marginal probabilities in distributions [26-28]. Hence, the structure of the factor graph consists of two nodes that represent the relationships between the factor node and the bit node. A factor node is connected to a bit node by an edge. In this work, a factor graph is used to describe the 3×3 matrix of 2-D interference channel according to Equation (2) for the message-passing algorithm which represents the relationship between factor node and bit node. The factor node represents the received read-back signals, and the bit node represents the input bits. An edge is connected between a factor node and a bit node by using a posteriori log-likelihood ratio (LLR) information [25], [32]. Therefore, the essentials of the FGB detection lie in two steps at each iteration: the first step is that each factor node passes its priori information to the connected bit nodes, and the second step is that each bit node updates its a posteriori information according to the incoming information and then passes it back to each factor node. Furthermore, we observe from Eq. (2) that the 3×3 matrix of the 2-D interference channel is very complex in terms of the number of edges between the factor nodes and the bit nodes. Consequently, to avoid 2-D signal processing with the complexity, the 3×3 matrix of the 2-D interference channel is reshaped into a 1-D data array with the sequential order before sending it to the detector.

For a regular FGB detection, a region graph is formed using this partial ordering, which is the message-passing on the factor graph of the 2-D interference channel. For example, a factor node $[r_{j,k}]$ passes the messages to the connected nine bit nodes $[a_{j-1,k-1}, a_{j-1,k}, a_{j-1,k+1}, a_{j,k-1}, a_{j,k}, a_{j,k+1}, a_{j+1,k-1}, a_{j+1,k}, a_{j+1,k+1}]$, as shown in Fig. 2. Before sending the LLR information, each factor node computes the reliability information based on the read-back signals. When bit nodes received the information from the factor node, they $[a_{j-1,k-1}, a_{j-1,k}, a_{j-1,k+1}, a_{j,k-1}, a_{j,k}, a_{j,k+1}, a_{j+1,k-1}, a_{j+1,k}, a_{j+1,k+1}]$ updated and sent back the information to the connected eight factor nodes $[r_{j-1,k-1}, r_{j-1,k}, r_{j-1,k+1}, r_{j,k-1}, r_{j,k+1}, r_{j+1,k-1}, r_{j+1,k}, r_{j+1,k+1}]$, excluding the factor node $[r_{j,k}]$, as shown in Fig.3.

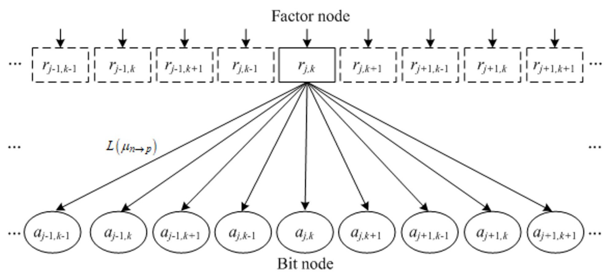


***Fig. 2**: The structure of factor graph in 2-D interference channel for message-passing of factor node connected to bit nodes.*

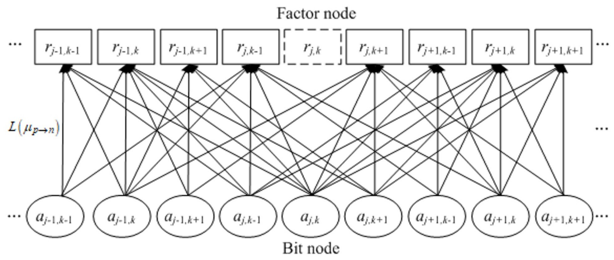


***Fig. 3**: The structure of factor graph in 2-D interference channel for message-passing of bit nodes connected to factor nodes.*

In constructing the FGB detection based on a 2-D interference channel that can be formulated as a convex optimization problem. An FGB detection provides a method to approximate marginal distributions, which makes it suitable for the MAP (maximum a posteriori probability) algorithm. The MAP algorithm is devised to minimize the bit probability and to provide reliability values of the decoded bits, which is the heart of iterative decoding [25-27]. In FGB detection, the message sent from form factor nodes $n$ to bit nodes $p$ is a posteriori probability that estimates each received signal bit by computing its log-likelihood ratio (LLR) $L(\mu_{n\to p})$, which is defined as

$$L\left(\mu_{n\to p}\right) = \log \frac{\Pr\left(a_n = +1|y_n\right)}{\Pr\left(a_n = -1|y_n\right)} = \log \frac{\sum_{C^n;x_p=+1} \Pr\left(y_n|C^n_{\sim x_p}, x_r = +1\right)\Pr\left(C^n_{\sim x_p}\right)}{\sum_{C^n;x_p=+1} \Pr\left(y_n|C^n_{\sim x_p}, x_r = -1\right)\Pr\left(C^n_{\sim x_p}\right)} \quad (5)$$

Next, formulate from Equation (5) to further simplify the computation; the log-MAP algorithm can be used, i.e.

$$L\left(\mu_{n\to p}\right) = \log \frac{\sum_{C^n;x_p=+1} \exp\left(-\frac{(r_n-y_n)^2}{2\sigma^2} + \sum_{r\in C^n_{\sim x_p}, x_r=+1} L\left(\mu_{r\to n}\right)\right)}{\sum_{C^n;x_p=-1} \exp\left(-\frac{(r_n-y_n)^2}{2\sigma^2} + \sum_{r\in C^n_{\sim x_p}, x_r=-1} L\left(\mu_{r\to n}\right)\right)} \quad (6)$$

where $r_n$ is the read-back signal with AWGN noise, $y_n$ is the received signal without noise, $\sigma^2$ is the variance of an AWGN, and LLR information $L(\mu_{r\to n})$ is used as the message sent from the bit node $r$ to the factor node $n$.

In the opposite direction, each bit node receives the LLR information from the factor nodes. The LLR of a posteriori probability of the signal is used as the information sent from bit nodes $p$ to factor nodes $n$. Therefore LLR $L(\mu_{p\rightarrow \mathrm{n}})$ can be calculated as

$$L\left(\mu_{p\rightarrow n}\right) = \sum_{r\in D_n^p} L\left(\mu_{r\rightarrow p}\right) \tag{7}$$

where $D_n^p$ is the set of factor nodes connected to the bit node $a_p$ excluding the factor node $r_n$.

In the first iteration, to proceed with the computation of the LLR information, $L(\mu_{p\rightarrow \mathrm{n}})$ is initialized to zero due to all the input bits, which are considered possible values. From the second iteration onwards, the factor nodes will update the information by using the new incoming LLR information $L(\mu_{r\rightarrow n})$. These updating information processes will continue until the last iteration is reached. After a specified number of iterations, the output of LLR information is given by

$$L\left(\hat{a}_n\right) = \sum L\left(\mu_{r\rightarrow n}\right) \tag{8}$$

Finally, the estimated data bit $L\left(\hat{a}_n\right)$ is then given by the sign of its LLR as follows:

$$\hat{a}_n = \begin{cases} +1, & \text{if } L\left(\hat{a}_n\right) \geq 0 \\ -1, & \text{otherwise} \end{cases} \tag{9}$$

### 3.1 Improved Factor Graph-Based (FGB) Decoder

In the BPMR channel, the 2-D interference channel has been considered as a useful scheme to increase efficiency in signal processing for communication of the BPMR channel. In this work, we will divide the recording channel into two channels that modify the coefficients of the 2-D interference channel based on the upper triangular matrix and lower triangular matrix. The coefficients of the 2-D interference channel represent the weights of the current channel from Equation (2). When we just use an upper triangular matrix for the coefficients of a 2-D interference channel. For convenience, the 2-D interference channel can be written as an upper triangular target ($\mathbf{H}_u$) of a 3×3 matrix as

$$\mathbf{H}_u = \begin{bmatrix} h_{j-1,k-1} & h_{j,k-1} & h_{j+1,k-1} \\ h_{j-1,k} & h_{j,k} & 0 \\ h_{j-1,k+1} & 0 & 0 \end{bmatrix}.$$

Therefore, the relationships of message-passing between factor nodes and bit nodes on the factor graph are according to Equations (6)-(9). From the factor graph considerations in Fig. 4, the 2-D interference channel with upper triangular ($\mathbf{H}_u$) shows the structure of the factor graph, which the factor graph as a read-back signal $[r_{j-1,k-1}, r_{j-1,k}, r_{j-1,k+1}, r_{j,k-1}, r_{j,k}, r_{j+1,\ k-1}]$ are sent the message to the connected bit nodes $[a_{j-1,k-1}, a_{j-1,k}, a_{j-1,k+1}, a_{j,k-1}, a_{j,k}, a_{j,k+1}, a_{j+1,\ k-1}, a_{j+1,k}, a_{j+1,k+1}]$. When all bit nodes in the channel received the information from factor nodes. Next, the bit node

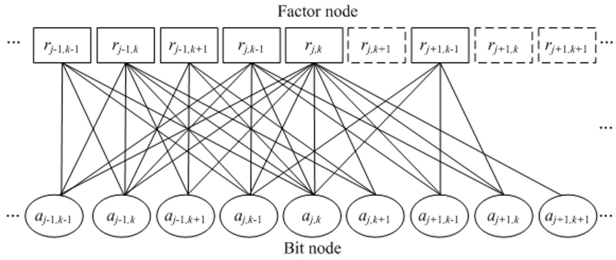


***Fig. 4****: The structure of factor graph for message-passing on 2-D interference channel with upper triangular.*

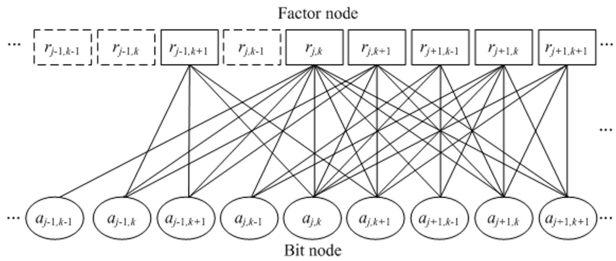


***Fig. 5****: The structure of factor graph for message-passing on 2-D interference channel with lower triangular.*

$[a_{j-1,k-1}, a_{j-1,k}, a_{j-1,k+1}, a_{j,k-1}, a_{j,k}, a_{j,k+1}, a_{j+1,k-1}, a_{j+1,k}, a_{j+1,k+1}]$ updates the information and sends it to the connected factor nodes $[r_{j-1,\ k-1}, r_{j-1,k}, r_{j-1,k+1}, r_{j,k-1}, r_{j,k}, r_{j+1,\ k-1}]$ except for the factor nodes $[r_{j,k+1}, r_{j+1,k}, r_{j+1,k+1}]$.

Similarly, for the 2-D interference channel with lower triangular target ($\mathbf{H}_l$), it can be written as

$$\mathbf{H}_l = \begin{bmatrix} 0 & 0 & h_{j+1,k-1} \\ 0 & h_{j,k} & h_{j+1,k} \\ h_{j-1,k+1} & h_{j,k+1} & h_{j+1,k+1} \end{bmatrix}.$$

Hence, we consider the factor graph on a 2-D interference channel with a lower triangular ($\mathbf{H}_l$) structure, which shows the message-passing on the factor graph. Factor nodes $[r_{j-1,k+1}, r_{j,k}, r_{j,k+1}, r_{j+1,\ k-1}, r_{j+1,k}, r_{j+1,k+1}]$ send the information to connect the bit nodes $[a_{j-1,k-1}, a_{j-1,k}, a_{j-1,k+1}, a_{j,k-1}, a_{j,k}, a_{j,k+1}, a_{j+1,k-1}, a_{j+1,k}, a_{j+1,k+1}]$. Then, bit nodes $[a_{j-1,k-1}, a_{j-1,k}, a_{j-1,k+1}, a_{j,k-1}, a_{j,k}, a_{j,k+1}, a_{j+1,k-1}, a_{j+1,k}, a_{j+1,k+1}]$ propagate updated information to the connected factor nodes $[r_{j-1,k+1}, r_{j,k}, r_{j,k+1}, r_{j+1,\ k-1}, r_{j+1,k}, r_{j+1,k+1}]$ but will not send the information back to the factor nodes $[r_{j-1,k-1}, r_{j-1,k}, r_{j,k-1}]$, as shown in Fig. 5.

### 3.2 A Combination of the FGB Detectors

For FGB detector design, we will refer to the two targets with the upper triangular and the lower triangular targets. Two FGB detection make the signal be in the form of known levels of the given 2-D interference channel with upper triangular and lower triangular. From block diagram considerations in Fig. 6, which illustrates an input bits sequence into two FGB detectors. When the output bit $z(u)_{j,k}$ of the 2-D equalizer (upper

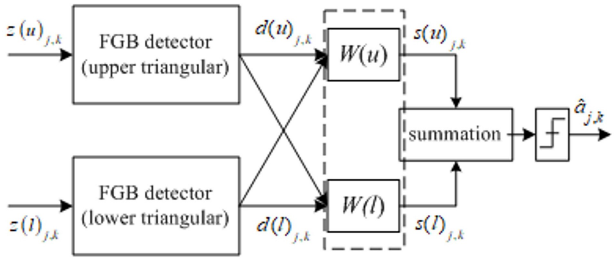


***Fig. 6****: Block diagram of a combination of FGB detectors.*

triangular) goes into the FGB detector (upper triangular) and the output bit $z(l)_{j,k}$ of the 2-D equalizer (lower triangular) goes into the FGB detector (lower triangular). After that, each output from two detectors is combined for input bit $\hat{a}_{j,k}$.

In the following analysis, we simplify the improved FGB detection method, which uses a soft output detection scheme. Consequently, if each output of two detections $d(u)_{j,k}$ and $d(l)_{j,k}$ is a summation of the weighted value $W(u)$ by using the relation

$$W(u) = \frac{d(u)_{j,k}}{d(u)_{j,k} + d(l)_{j,k}} \tag{10}$$

In the same manner, the weighted value $W(l)$ can be written as

$$W(l) = \frac{d(l)_{j,k}}{d(u)_{j,k} + d(l)_{j,k}} \tag{11}$$

where $d(u)_{j,k}$ and $d(l)_{j,k}$ are the output bits from two FGB detectors in the upper triangular and lower triangular parts, respectively.

When the corresponding output value $s(u)_{j,k}$ is defined as

$$s(u)_{j,k} = d(u)_{j,k} \times W(u) \tag{12}$$

Consequently, the output value $s(u)_{j,k}$ is given as

$$s(l)_{j,k} = d(l)_{j,k} \times W(l) \tag{13}$$

From these relations, it is easy to show that the input bit $\hat{a}_{j,k}$ estimation is a combination of $s(u)_{j,k}$ and $s(l)_{j,k}$ output values from both weighted values. Therefore, the final input bit $\hat{a}_{j,k}$ estimation is then given by

$$\hat{a}_{j,k} = s(u)_{j,k} + s(l)_{j,k} \tag{14}$$

where $s(u)_{j,k}$ and $s(l)_{j,k}$ are the output bits from the weighted values $W(u)$ and $W(l)$ of two FGB detectors with upper triangular and lower triangular, respectively.

Since this can be further illustrated if a basic input bit $\hat{a}_{j,k}$ estimation is obtained in the form

$$\hat{a}_{j,k} = \begin{cases} +1, & \text{if } \hat{a}_{j,k} \geq 0 \\ -1, & \text{otherwise} \end{cases} \tag{15}$$

## 4. RESULTS AND DISCUSSIONS

In the following analysis, we consider the BPMR channel with an areal density of 3 and 4 Tb/in$^2$ [21-22], [31]. For our simulation parameters, the bit period ($T_x$ ) and the track pitch ($T_z$ ) are 13.2 nm for an areal density of 3 Tb/in$^2$. Hence, an areal density of 4 Tb/in$^2$, the parameters of $T_x$ and $T_z$ are 12.7 nm, which sets the similar parameters of $PW_{50x}$ along the track and $PW_{50z}$ across the track at 4.2 nm and 8.4 nm, respectively. In order to facilitate this work, the 2-D interference channel matrix $\mathbf{H}$ with the size of 3×3 can be written as

$$\mathbf{H}_{3Tb} = \begin{bmatrix} 0.0117 & 0.3724 & 0.0117 \\ 0.0315 & 1.0000 & 0.0315 \\ 0.0117 & 0.3724 & 0.0117 \end{bmatrix},$$

and

$$\mathbf{H}_{4Tb} = \begin{bmatrix} 0.0163 & 0.4008 & 0.0163 \\ 0.0408 & 1.0000 & 0.0408 \\ 0.0163 & 0.4008 & 0.0163 \end{bmatrix}.$$

The introduction of data bits of the BPMR channel is read in the form of a 2-D page with 1,024×1,024 arrays. Following this approach, the 3×7 matrix of the 2-D equalizer is designed based on the minimum-mean-squared-error (MMSE) [34-36]. The signal-to-noise ratio (SNR) for channels can thus be defined as

$$SNR = 10\log_{10}\left(\frac{E_p}{\sigma^2}\right).$$

where $E_p = 1$ is the peak signal of the read-back signal and the $\sigma$ is the additive white Gaussian (AWGN) noise.

In Fig. 7, we compare the BER performance of the improved FGB detector with one to four iterations on the BPMR channel at an areal density of 3 Tb/in$^2$. From simulation, the improved FGB detector with three iterations has a similar BER performance as the four iterations.

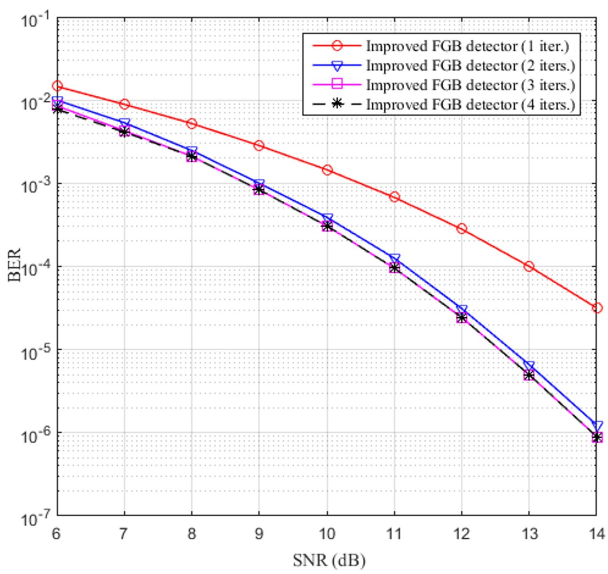


***Fig. 7****: BER performance of improved FGB detector with one to four iterations on BPMR channel at areal density 3 Tb/in$^2$.*

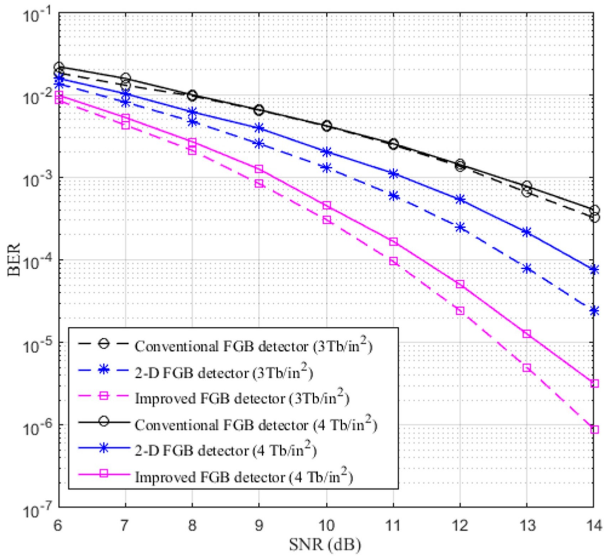


***Fig. 8**: BER performance comparison of improved FGB detector, FGB detector and 2-D FGB detector at three iterations.*

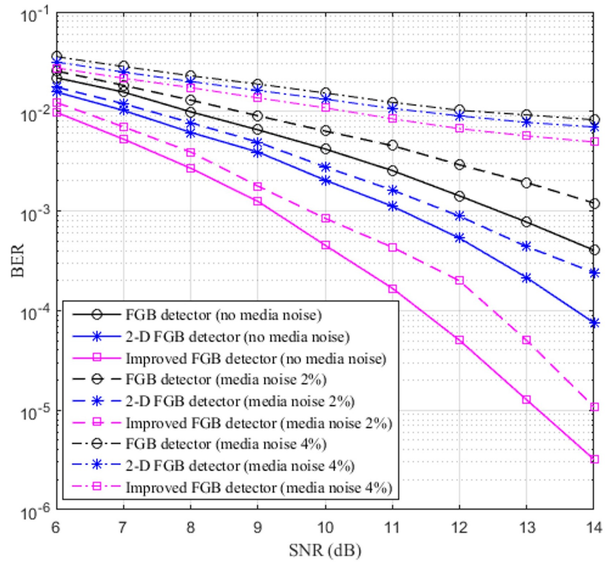


***Fig. 9**: BER performance comparison of improved FGB detector, FGB detector, and 2-D detector on the BPMR channel at an areal density of 4 Tb/in$^2$ with media noises.*

Figure 8 shows the BER performance results for the BPMR channel with an areal density of 3 and 4 Tb/in$^2$. We compare the BER performance of three detectors, which consist of an improved FGB detector, an FGB detector, and a 2-D FGB detector. In simulation, the BER performance of the improved FGB detector has more gains compared with the 2-D FGB detector and the conventional FGB detector. For example, when we consider the BPMR channel with an areal density of 4 Tb/in$^2$, the BER performance of an improved FGB detector is better than the conventional FGB detector in SNR of 4 dB at BER =$10^{-4}$. Moreover, an improved FGB detector achieves a gain of about 2.2 dB over the 2-D FGB detector at BER =$10^{-5}$ at three iterations, because the BER performance of the four iterations is similarly three iterations.

In Fig. 9, we plot the BER curves versus SNR, which evaluate the BER performance of each FGB detector under the presence of the BPMR channel at an areal density of 4 Tb/in$^2$ with media noises. Media noise indicates the effect of the size fluctuation and position fluctuation in along-track and across-track directions at 2% and 4%, respectively. From results simulation, we observe that as media noise increases, significant BER performance of each FGB detector deterioration is incurred.

## 5. CONCLUSIONS

In this work, we have proposed improved FGB detection from a 2-D interference channel based on a factor graph in the BPMR system with an areal density of 3 and 4Tb/in$^2$. A 2-D interference channel is segmented into two targets as upper triangular and lower triangular factor graphs. Simulation results show the BER performance that the proposed improved FGB detector has more gains compared with the conventional FGB detector and 2-D FGB detector. Moreover, an improved FGB detector is better than an FGB detector and a 2-D FGB detector on the BPMR channel with media noise. Since the usefulness of the model is seen from its application to capacity design and evaluation of optimized detection schemes, which should reliably reflect the detection processes of the 2-D interference channel. But potentially have different detection and operate at different 2-D interference channels to areal densities.

## ACKNOWLEDGEMENT

This work was supported in part by the Department of Electronics Engineering, Faculty of Engineering and Technology, Rajamangala University of Technology Isan, Nakhon Ratchasima, Thailand, and in part by the Office of the Higher Education Commission and the Thailand Research Fund under Grant MRG6180092.

## REFERENCES

[1] G. F. Hughes, “Read Channels for Patterned Media,” *IEEE Transactions on Magnetics*, vol. 35, no. 5, pp. 2310-2312, Sep. 1999.

[2] R. Wood, “The Feasibility of Magnetic Recording at 1 Terabit per Square Inch,” *IEEE Transactions on Magnetics*, vol. 36, no. 1, pp. 36-42, Jan. 2000.

[3] H. J. Richter, A. Y. Dobin, O. Heinonen, K. Z. Gao, R. J. M. v. d. Veerdonk, R. T. Lynch, J. Xue, D. Weller, P. Asselin, M. F. Erden, and R. M. Brockie, “Recording on Bit-Patterned Media at Densities of 1 Tb/in$^2$ and Beyond,” *IEEE Transactions on Magnetics*, vol. 42, no. 10, pp. 2255-2260, Oct. 2006.

[4] A. Kikitsu, “Prospects for bit patterned media

for high-density magnetic recording," *Journal of Magnetism and Magnetic Materials*, vol. 321, no. 6, pp. 526-530, Mar. 2009.

[5] H. Saito, "Signal-Processing Schemes for Multi-Track Recording and Simultaneous Detection Using High Areal Density Bit-Patterned Media Magnetic Recording," *IEEE Transactions on Magne*tics, vol. 51, no. 11, ID. 3101404, Nov. 2015.

[6] N. Honda, K. Yamakawa, J. Ariake, Y. Kondo, and K. Ouchi, "Write Margin Improvement in Bit Patterned Media With Inclined Anisotropy at High Areal Densities," *IEEE Transactions on Magnetics*, vol. 47, no. 1, pp. 11-17, Jan. 2011.

[7] H. Muraoka, and S. J. Greaves, "Statistical Modeling of Write Error Rates in Bit Patterned Media for 10 Tb/in$^2$ Recording," *IEEE Transactions on Magnetics*, vol. 47, no. 1, pp. 26-34, Jan. 2011.

[8] S. J. Greaves, Y. Kanai, and H. Muraoka, "Magnetic Recording in Patterned Media at 5-10 Tb/in$^2$," *IEEE Transactions on Magnetics*, vol. 44, no. 11, pp. 3430-3433, Nov. 2008.

[9] S. Wang, Y. Wang and R. H. Victora, "Shingled Magnetic Recording on Bit Patterned Media at 10 Tb/in$^2$," *IEEE Transactions on Magnetics*, vol. 49, no. 1, pp. 3644-3647, Jul. 2013.

[10] S. Nabavi, B. V. K. Vijaya Kumar, and J. G. Zhu, "Modifying Viterbi Algorithm to Mitigate Intertrack Interference in Bit-Patterned Media," *IEEE Transactions on Magnetics*, vol. 43, no. 6, pp. 2274-2276, Jun. 2007.

[11] W. Chang, and J. R. Cruz, "Inter-Track Interference Mitigation for Bit-Patterned Magnetic Recording," *IEEE Transactions on Magnetics*, vol. 46, no. 11, pp.3899-3908, Nov. 2010.

[12] P. W. Nutter, I. T. Ntokas, B. K. Middleton, and D. T Wilton, "Effect of Island Distribution on Error Rate Performance in Patterned Media," *IEEE Transactions on Magnetics*, vol. 41, no. 10, pp. 3214-3216, Oct. 2005.

[13] S. Nabavi, B. V. K. Vijaya Kumar, and J. A. Bain, "Two-Dimensional Pulse Response and Media Noise Modeling for Bit-Patterned Media," *IEEE Transactions on Magnetics*, vol. 44, no. 11, pp. 3789-3792, Nov. 2008.

[14] P. W. Nutter, I. T. Ntokas, and B. K. Middleton, "An Investigation of the Effects of Media Characteristics on Read Channel Performance for Patterned Media Storage," *IEEE Transactions on Magnetics*, vol. 41, no. 11, pp. 4327-4334, Nov. 2005.

[15] Y. Wang, J. Yao, and B. V. K. Vijaya Kumar, "2-D Write/Read Channel Model for Bit-Patterned Media Recording With Large Media Noise," *IEEE Transactions on Magnetics*, vol. 51, no. 12, ID. 3002 611, Dec. 2015.

[16] Y. Shi, P. W. Nutter, B. D. Belle, and J. J. Miles "Error Event Due to Island Size Variations in Bit Patterned Media," *IEEE Transactions on Magnetics*, vol. 46, no. 6, pp. 1755-1758, Jun. 2010.

[17] L. Alink, J. P. J. Groenland, J. D. Vries, and L. Abelmann, "Determination of Bit Patterned Media Noise Based on Island Perimeter Fluctuations," *IEEE Transactions on Magnetics*, vol. 48, no. 11, pp. 4574-4577, Nov. 2012.

[18] J. Kim, and J. Lee, "Iterative Two-Dimensional Soft Output Viterbi Algorithm for Patterned Media," *IEEE Transactions on Magnetics*, vol. 47, no. 3, pp. 594-597, Mar. 2011.

[19] S. Karakulak, P. H. Siegel, J. K. Wolf, and H. N. Bertram, "Joint-Track Equalization and Detection for Bit Patterned Media Recording," *IEEE Transactions on Magnetics*, vol. 46, no. 9, pp. 3639-3647, Sep. 2010.

[20] C. D. Nguyen, and J. Lee, "Twin Iterative Detection for Bit-Patterned Media Recording Systems," *IEEE Transactions on Magnetics*, vol. 53, no. 11, ID. 8109 304, Nov. 2017.

[21] Y. Wang, B. V. K. Vijaya Kumar, "Improved Multitrack Detection With Hybrid 2-D Equalizer and Modified Viterbi Detector," *IEEE Transactions on Magnetics*, vol. 53, no. 10, ID.3000710, Oct. 2017.

[22] T. Wu, M. A. Armand and J. R. Cruz, "Detection-Decoding on BPMR Channels With Written-In Error Correction and ITI Mitigation," *IEEE Transactions on Magnetics*, vol. 50, no. 1, ID. 3000211, Jan. 2014.

[23] S. Jeong, and J. Lee, "Signal Detection Under Multipath Intersymbol Interference in Staggered Bit-Patterned Media Recording Systems," *IEEE Magnetics Letters*, vol.10, ID.6501005, Jan. 2019.

[24] T. A. Nguyen, and J. Lee, "Iterative Parallel-Serial Detection Structure Using MAP Algorithm for Bit-Patterned Media Recording Systems," *IEEE Transactions on Magnetics*, vol. 59, no. 3, ID. 30003 06, Mar. 2023.

[25] J. Hu and T. M. Duman, "Graph-Based Detector for BLAST Architecture," *in Proceedings of 2007 IEEE International Conference on Communications (ICC 2007)*, Glasgow, Scotland, pp. 1018-1023, 2007.

[26] J. Hu, T. M. Duman, M. F. Erden, "Graph-Based Channel Detection for Multitrack Recording Channels," *EURASIP Journal on Advances in Signal Processing*, doi: 10.1155/2008/738281, ID. 738281, pp. 1-9, Nov. 2008.

[27] T. Sopon, P. Supnithi, and K. Vichienchom, "Improved 2-D Graph-Based Detectors for 2-D Interference Channels," *IEEE Transactions on Magnetics*, vol. 50, no. 11, ID. 3101704, Nov. 2014.

[28] G. Colavolpe and G. Germi, "On the Application of Factor Graphs and Sum-Product Algorithm to ISI Channels," *IEEE Transactions on Communications*, vol. 53, no. 5, pp. 818–825, May 2005.

[29] S. M. Khatami, and B. Vasic, "Generalized Belief Propagation Detector for TDMR Microcell Model," *IEEE Transactions on Magnetics*, vol. 49, no. 7, pp. 3699-3702, Jul. 2013.

[30] J. S. Yedidia, W. T. Freeman, and Y. Weiss,

"Constructing Free-Energy Approximations and Generalized Belief Propagation Algorithms," *IEEE Transactions on Information Theory*, vol. 51, no. 7, pp. 2282-2312, Jul. 2005.

[31] Y. Ng, K. Cai, B. V. K. Vijaya Kumar, T. C. Chong, S. Zhang, and B. J. Chen, "Channel Modeling and Equalizer Design for Staggered Islands Bit-Patterned Media Recording," *IEEE Transactions on Magnetics*, vol. 48, no. 6, pp. 1976-1983, Jun. 2012.

[32] B. M. Kurkoski, P. H. Siegel, and J. K. Wolf, "Joint Message-Passing Decoding of LDPC Codes and Partial-Response Channels," *IEEE Transactions on Information Theory*, vol. 48, no. 6, pp. 1410-1422, Jun. 2002.

[33] J. Moon, and W. Zeng, "Equalization for Maximum Likelihood Detectors," *IEEE Transactions on Magnetics,* vol. 31, no. 2, pp. 1083–1088, Mar. 1995.

[34] S. Nabavi, and B. V. K. Vijaya Kumar, "Two-Dimensional Generalized Partial Response Equalizer for Bit-Patterned Media," *in Proceedings of 2007 IEEE International Conference on Communications (ICC 2007)*, Glasgow, Scotland, pp. 6249–6254, 2007.

[35] Y. Ng, K. Cai, B. V. K. Vijaya Kumar, S. Zhang and T. C. Chong, "Modeling and Two-Dimensional Equalization for Bit-Patterned Media Channels With Media Noise," *IEEE Transactions on Magnetics*, vol. 45, no. 10, pp. 3535-3538, Oct. 2009.

[36] K. Koo, S. Y. Kim, J. J. Jeong, and S. W. Kim, "Two-Dimensional Soft Output Viterbi Algorithm With Dual Equalizers for Bit-Patterned Media," *IEEE Transactions on Magnetics*, vol. 49, no. 6, pp. 2555–2558, Jun. 2013.

**Thanomsak Sopon** received the B.Eng.degree in Electronics Engineering from Sripatum University, Bangkok, Thailand, in 1998, the M.Eng. degree in Computer Engineering from Khon Kaen University, Khon Kaen, Thailand, in 2010, and the Ph.D. degree in Data Storage Technology from the King Mongkut's Institute of Technology Ladkrabang, Bangkok, Thailand, in 2014. In 2017, he has been an Assistant Professor at Department of Electronics Engineering, Faculty of Engineering and Technology, Rajamangala University of Technology Isan, Nakhon Ratchasima, Thailand. His research interests include data storage technology, digital communications, digital signal processing, and artificial intelligence.

**Pornchai Supnithi** received the B.S. degree from the University of Rochester, Rochester, NY, USA, in 1995, the M.S. degree from the University of Southern California, Los Angeles, CA, USA, in 1997, and the Ph.D. degree in electrical Engineering from the Georgia Institute of Technology, Atlanta, GA, USA, in 2002. Since 2015, he has been a full professor at Telecommunication Engineering Department, Faculty of Engineering, King Mongkut's Institute of Technology Ladkrabang. He has published over 50 journal articles, 100 conference papers, and 3 books/chapters. His research interests are in the area of Telecommunications, Ionospheric and GNSS, Data storage, and Engineering Education. His laboratory is maintaining numerous observation stations in Thailand (with ionosonde, beacon receivers, magnetometer, and GNSS receivers) as well as Thai GNSS and Space Weather Information Website (http://iono-gnss.kmitl.ac.th). Prof. Dr. Pornchai Supnithi was a mid-career Thailand Research Fund scholar from 2013-2015. He previously served as the second Vice President of ECTI Association. Currently, he serves as a subcommittee member in the National Research Council of Thailand (NRCT), International Reference Ionosphere (IRI) Committee (under URSI, COSPAR), and the National GNSS Infrastructure subcommittee, Ministry of Science and Technology, Thailand.